Fast Response Organic Supramolecular Transistors Utilizing In-Situ π-Ion Gels

Soh Kushida, Emanuel Smarsly, Kyota Yoshinaga, Irene Wacker, Yohei Yamamoto, Rasmus R. Schröder, and Uwe H. F. Bunz**

Despite their remarkable charge carrier mobility when forming well-ordered fibers, supramolecular transistors often suffer from poor processability that hinders device integration, resulting in disappointing transconductance and output currents. Here, a new class of supramolecular transistors, π-ion gel transistors (PIGTs), is presented. An in situ π-ion gel, which is an unprecedented composite of semiconducting nanofibers and an enclosed ionic liquid, is directly employed as an active material and internal capacitor. In comparison to other supramolecular transistors, a PIGT displays a high transconductance (133 μS) and output current (139 μA at –6 V), while retaining a high charge-carrier mobility (4.2×10^{-2} cm^2 V^{-1} s^{-1}) and on/off ratio (3.7×10^4). Importantly, the unique device configuration and the high ionic conductivity associated with the distinct nanosegregation enables the fastest response among accumulation-mode electrochemical-based transistors (<20 μs). Considering the advantages of the absence of dielectric layers and the facile fabrication process, PIGT has great potential to be utilized in printed flexible devices. The device platform is widely applicable to various supramolecular assemblies, shedding light on the interdisciplinary research of supramolecular chemistry and organic electronics.

Molecular self-assembly can create more sophisticated structures of minute dimensions than any artificial engineering.[1] In particular, assemblies of π-conjugated molecules are intriguing due to the critical impact on their optoelectronic properties.[2] One example is gels composed of π-conjugated molecules (π-gels).[3] π-Gels are nanocomposites that comprise branched fibers and enclosed solvents. In the fibers, π-conjugated molecules typically assume polycrystalline ordering. Since the charge transport in organic semiconductors is governed by intermolecular interactions, the high crystallinity of π-gels provides preferable electronic properties. π-Gels have been applied to a variety of electronic devices including organic field-effect transistors (OFETs).[4] These supramolecular devices display improved performance in comparison to that of bulk devices. However, integrating supramolecular assemblies into a device still remains elusive, that is, transforming a gel to a device often results in sparsely dispersed fibers. Although individual molecular assemblies display remarkable charge-carrier mobility, the transconductance ($g_\mathrm{m} = \partial I_\mathrm{d}/\partial V_\mathrm{g}$) and the output current by the device unit are far below the practically desired values.

Recently, we comprehensively studied the gelation behavior of poly(*para*-phenyleneethynylene)s (PPEs) and disclosed a method to create an unprecedented π-gel containing an ionic liquid (IL) instead of a solvent (π-ion gel).[5] The space-filling IL and semiconducting fibers are independently bicontinuous, thus, π-ion gels are not only electrically, but also ionically conductive. This structural design enabled further applications of π-gels to electrochemical-based devices.

Organic electrochemical transistors (OECTs) are transistors that involve electrochemical doping.[6] Although the device configuration of OECTs is identical to that of electrolyte-gate OFETs, the principal mechanism differs fundamentally. Once a gate bias is applied, ions pass through the boundary and penetrate the active layer. As a result, the whole layer is electrochemically doped, gaining a volumetric current through the full, 3D channel. In comparison to OFETs, where currents flow only at the interface of the semiconductor, OECTs exhibit output currents and transconductances that are several orders of magnitude higher. However, the response speed of OECTs is typically slow due to the co-occurring events of ion penetration and subsequent doping. In 2019, an ultrafast-responding (≈2.6 μs) depletion-mode OECT, which is driven via dedoping of poly(3,4-ethylenedioxythiophene) polystyrene sulfonate, was achieved with a narrow channel fabricated

---

Dr. S. Kushida, Dr. E. Smarsly, Prof. U. H. F. Bunz
Organisch-Chemisches Institut
Ruprecht-Karls-Universität Heidelberg
Heidelberg INF 270 69120, Germany
E-mail: s-kushida@ims.tsukuba.ac.jp; uwe.bunz@oci.uni-heidelberg.de

Dr. S. Kushida, Dr. I. Wacker, Prof. R. R. Schröder, Prof. U. H. F. Bunz
Centre for Advanced Materials (CAM)
Ruprecht-Karls-Universität Heidelberg
Heidelberg INF 225 69120, Germany

Dr. S. Kushida, K. Yoshinaga, Prof. Y. Yamamoto
Faculty of Pure and Applied Sciences, and Tsukuba Research Center for Energy Materials Science (TREMS)
University of Tsukuba
1-1-1 Tennoudai, Tsukuba 305-8573, Japan

The ORCID identification number(s) for the author(s) of this article can be found under https://doi.org/10.1002/adma.202006061.

DOI: 10.1002/adma.202006061

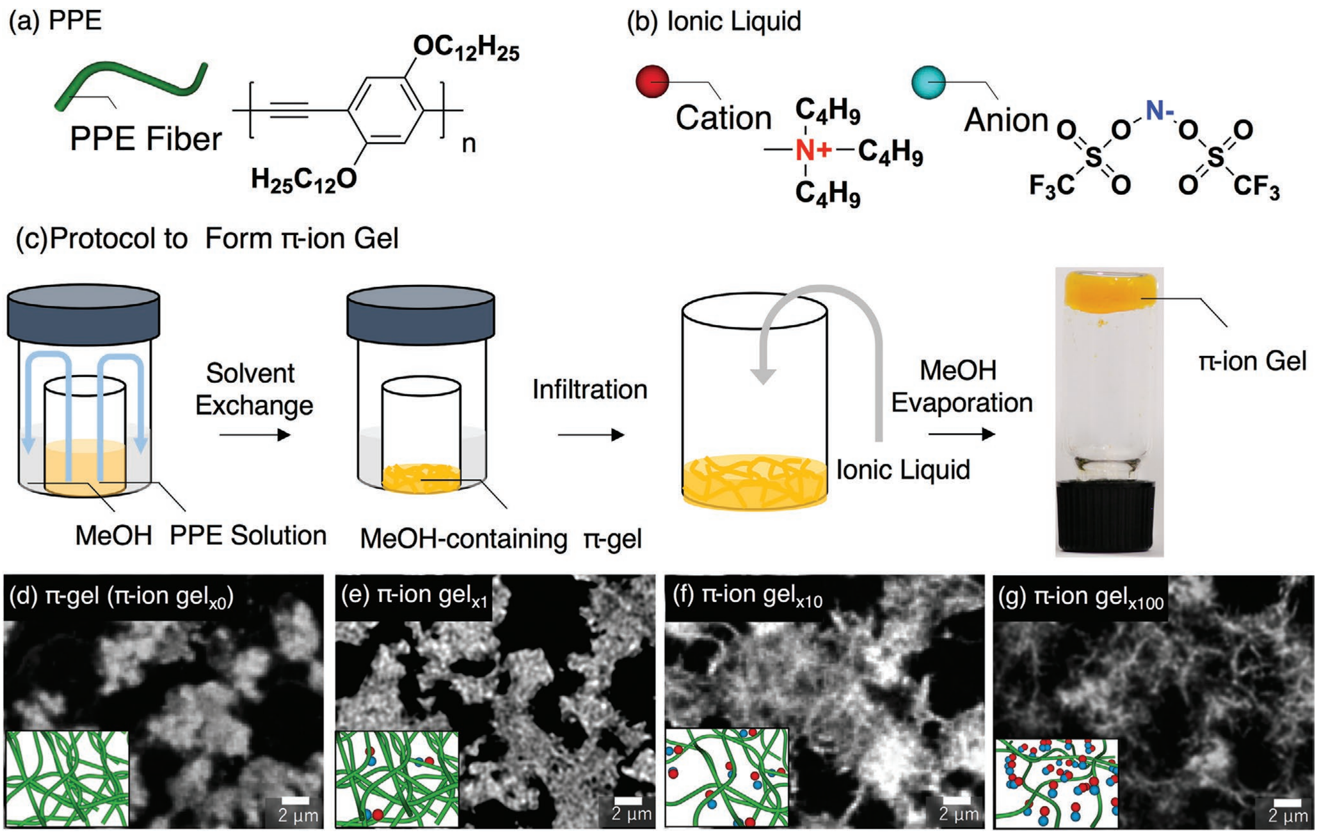

Figure 1. Schematic illustrations and chemical structures of the a) PPE and b) IL utilized in this work. c) Fabrication protocol of π-ion gel: THF in the PPE solution is replaced with methanol via solvent exchange to obtain a π-gel containing methanol. Infiltration of the IL and subsequent removal of methanol via spontaneous evaporation results in the formation of the π-ion gel. Confocal fluorescence microscopy (CFM) images of π-gels containing different amounts of IL: d) π-ion gel$_{x0}$, e) π-ion gel$_{x1}$, f) π-ion gel$_{x10}$, and g) π-ion gel$_{x100}$ after evacuation. The insets show schematic images of the most likely nanostructures.

by photolithography.[6i] Yet, accumulation-mode OECTs, which are driven via doping of neutral semiconductors, are operative at ≈1 ms at best,[6f] thus hindering potential applications.

In this paper, we present a new class of supramolecular transistors, named π-ion gel transistors (PIGTs), that employ an in situ π-ion gel as an active layer as well as an internal gate capacitor. PIGTs exhibit a large transconductance of 133 µS, retaining a hole carrier mobility (4.2×10^{-2} cm^2 V^{-1} s^{-1}) and an on/off ratio ($\approx 3.7 \times 10^4$) comparable to those of supramolecular devices. Due to the unique device structure, PIGT shows a response time of <20 µs, the fastest time among accumulation-mode electrochemical-based transistors ever reported.

The formation of the π-ion gel was published in our previous research (**Figure 1**c).[5] A conjugated polymer, dihexyl-PPE (Figure 1a), formed a π-gel through solvent exchange from tetrahydrofuran to methanol. The π-gel consists of fibers with a diameter below one hundred nanometers, as seen in the scanning electron microscopy (SEM) image (Figure S1a, Supporting Information). It was also confirmed that the solvent content in the π-gel was 90% methanol in our previous study.[5a] This is critical for facilitating compatibility with ILs. In the second step, a variable amount of IL was infiltrated into the π-gel. Subsequently, methanol was removed by spontaneous evaporation, resulting in the formation of the π-ion gel. As an IL, tributylmethylammonium bis(trifluoromethanesulfonyl-)imide (Figure 1b) was employed. Depending on the amount of infiltrated IL, π-ion gels with 0, 1, 10, and 100 weight ratios of IL are named π-ion gel$_{x0}$, π-ion gel$_{x1}$, π-ion gel$_{x10}$, and π-ion gel$_{x100}$, respectively. The fine structure of π-ion gels was not visible by SEM because the space between the fibers was filled with the IL and no topology was detectable (Figure S1b–d, Supporting Information). To elucidate the internal structures, we performed confocal fluorescence microscopy (CFM) (Figure 1d–g). Since PPE is fluorescent at 650 nm, a clear contrast between PPE and IL could be observed even with a limited spatial resolution of 200 nm. PPE fibers and IL are bicontinuously segregated, and the fibers enclose the IL in π-ion gel$_{x100}$ (Figure 1g). As the IL ratio decreased, the PPE fibers became dense, as seen in the SEM and CFM micrographs of other π-ion gels, indicating that the PPE fiber network shrank depending on the amount of IL intercalated into the space that was previously filled with methanol (Figure 1e–g; Figure S1, Supporting Information). It is remarkable that only 1% PPE encloses 99% IL and still retains its gel conformation in π-ion gel$_{x100}$. A film containing such a high amount of IL cannot be accessed by spin-coating or by drop-casting techniques. These methods result in the dispersed PPE aggregates in the IL rather than homogeneous films (Figure S2, Supporting Information).

The device structure of a PIGT is shown in **Figure 2**a. Its fabrication process is straightforward as only the formation of a π-ion gel on a substrate with prepatterned electrodes is required. The gate is an external needle located next to the contacts.

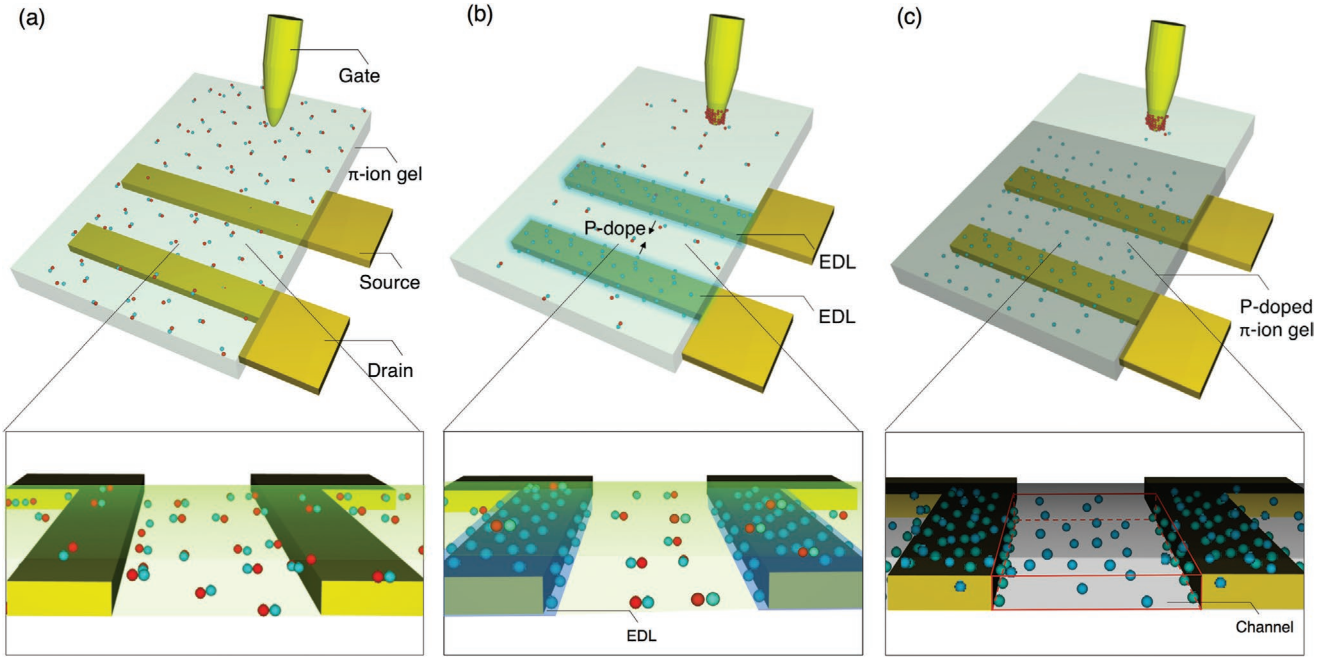

Figure 2. Suggested functional mechanism of PIGT. a) Device structure of PIGT. Once a gate voltage is applied, ions dissociate and form electric double layers (EDL) on contacts, b) allowing charge carrier injection. The c) whole gel is electrochemically doped, and the channel becomes 3D conductive.

Stacking a dielectric layer is not required because the internal IL works as an internal capacitor (for a detailed protocol, see the Experimental Section). The suggested functional mechanism is as follows: Once the gate is negatively biased, interior cations and anions move to the gate and contacts, respectively. Electric double layers form at the boundary of the contacts and the *π*-ion gel, allowing ohmic contact (Figure 2b). The ohmic contact induces *p*-doping of PPE, and the doped region is compensated and stabilized by an excess number of anions. The *p*-doping starts at the contacts and expands to the entire gel as is evident from the black color of the doped devices (Figure 2c; Figure S3, Supporting Information). Therefore, volumetric conductivity is expected as well as OECTs.[6]

To gain proof of volumetric conductivity, PIGTs composed of *π*-ion gel$_{x100}$ (PIGT$_{x100}$) were fabricated with variable thicknesses. The channel is defined by three parameters: the width (W), the length (L), and the thickness (T) (**Figure** 3a). Here, W and L were fixed at 2 mm and 40 µm, respectively. T was varied to 50, 90, 130, and 180 nm. The transfer curves of the drain currents (I_d) over the gate voltages (V_g) with variable contact thicknesses are shown (Figure 3b). The threshold of the gate voltage (V_{th}) of PIGT lies at −5 V regardless of T, whereas I_d depends on T. It can be decreased further by utilizing U-shaped gate contacts (Figure S4, Supporting Information). PIGT$_{x100}$ displays an on/off of ≈10^4 at V_g of ($-1 + V_{th}$) V. The detailed parameters are summarized in Table S1, Supporting Information. The transconductance ($g_m = \partial I_d/\partial V_g$) was obtained from four transistors for each thickness and is plotted as a function of T (Figure 3c). The transconductance and T are proportional, indicating the presence of volumetric conductivity in the channel. The obtained transconductance is 100 times larger than the best transconductance of an OFET built from the same PPE.[7a] However, this comparison is inappropriate for indicating which specific parameters are improved because the transconductance is amplified by the channel geometry or applied capacitance. To gain more insight into parameter improvement, the hole mobility (μ_{hole}) in the saturated regime was calculated according to the following equation for OECTs Equation (1).[6c,h]

$$g_m = \left(\frac{W\,T}{L}\right)\mu_{hole}\,C^*\left(V_g - V_{Th}\right) \tag{1}$$

where C^* is the volumetric capacitance. And a C^*value of 134.3 F cm^{-3} was determined by impedance measurements (**Figure** 4a). As seen in Figure 3d and Table S1, Supporting Information, μ_{hole} is invariant with T (3.2–4.2 × 10^{-2} cm^2 V^{-1} s^{-1}). The calculated μ_{hole} is equal to that of the self-assembled fiber OFETs (10^{-2}–10^{-1} cm^2 V^{-1} s^{-1}) and one order of magnitude higher than that of PPE-based OFETs (10^{-3}–10^{-2} cm^2 V^{-1} s^{-1}).[4e,7a] The output curves of PIGT$_{x100}$ are shown in Figure S5, Supporting Information. The output characteristic shows saturation of I_d, indicating a steady state. The gate current (I_g) is moderate (I_g/I_d = ≈5%) as shown in Figures S5 and S6, Supporting Information. It is fair to mention that PIGTs made of PPE display stable transconductance and output currents under continuous operation in N$_2$ while ambient atmosphere accelerates the degradation of PPE as *p*-doped PPE is known to be unstable (Figure S7, Supporting Information).[5b] The decrease of on/off ratios can be assigned to leakage of the channel at $V_g = 0$ caused by the remaining charge-carriers. It was also found that applying positive gate bias after each operation is effective to keep the high on/off ratios (Figure S7b, Supporting Information). We also mention that a limited amount of ILs can form *π*-ion gels due to the incompatibility toward *π*-gels. Figure S8, Supporting Information, shows the comparison of transconductances with various ILs available.

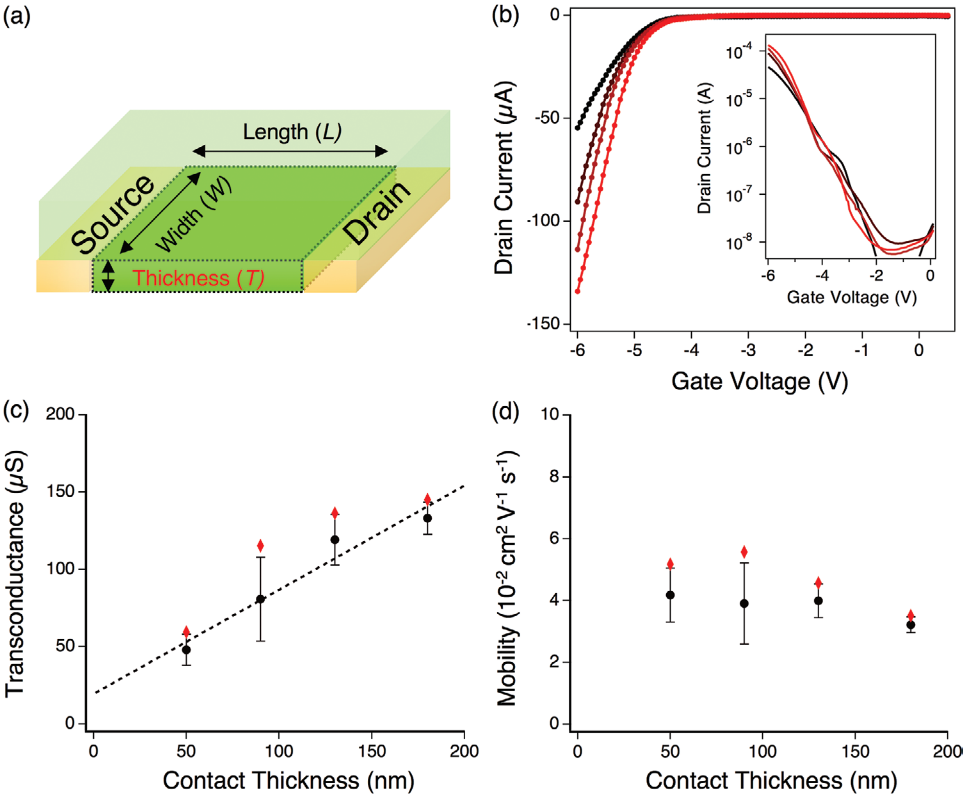

Figure 3. a) Definition of the dimensions of the channel. b) Transfer curves of PIGT$_{x100}$ with channel thicknesses of 50 nm (black), 90 nm (brown), 130 nm (dark red), and 180 nm (red). The inset displays the logarithmic drain currents over the gate voltage. The calculated c) transconductance and d) hole mobility as a function of the contact thickness. The black dots and red dots indicate the averaged values and maximum values, respectively.

The ratio of IL has a vital impact on device performance and response speed. The frequency-dependent capacitance of π-ion gel$_{x1}$, π-ion gel$_{x10}$, and π-ion gel$_{x100}$ without DC voltages refers to the response speed of ions in the gels as a high-ion-conductive material should have saturation and depletion points of capacitance at high frequencies (Figure 4a; Figure S9, Supporting Information). The saturation/depletion frequencies of π-ion gel$_{x100}$, π-ion gel$_{x10}$, and π-ion gel$_{x1}$ are 100 Hz/≈0.25 MHz, 2.5 Hz/≈0.25 MHz, and 80 mHz/5 kHz, respectively (Table S2, Supporting Information). This indicates that a high amount of IL enhances the ionic conductivity. In particular, π-ion gel$_{x100}$ shows comparable response to a pure IL. This result can be attributed to the structural morphology. The large space between the PPE network provides the conduction paths of ions and prevents the isolation of IL in the gel, maintaining a large interface between the fibers and ions. When a DC voltage is applied, the channel is electrochemically doped and its capacitance value drastically increases as a consequence of injected carriers, forming a volumetric capacitor. The capacitance is normalized by the channel volume, as shown in Figure 4a, inset, and Table S3, Supporting Information. The IL ratio has an impact on the C^* values because a certain number of anions are required to stabilize charge carriers in the channel.

The transfer curves of PIGTs as a function of the sweeping speed (0.1 s/step, 0.5 s/step, 1 s/step, and 5 s/step, step: 50 mV) and the resulting transconductance are shown in Figure S10, Supporting Information, and Figure 4b, respectively (other parameters, Table S4, Supporting Information). The transconductance of PIGT$_{x100}$ is independent of the sweeping speed. On the other hand, those of PIGTs composed of π-ion gel$_{x10}$ (PIGT$_{x10}$) and PIGTs composed of π-ion gel$_{x1}$ (PIGT$_{x1}$) drastically decrease with fast sweeping. Plotting transconductance ratio of PIGTs that is normalized by the values at 5 s per step highlights this observation even more clearly (Figure 4b, inset). This result reflects the response time of devices. PIGT$_{x10}$ and PIGT$_{x1}$ require more time for ion redistribution and doping to reach a conductive steady-state due to the poor ion conductivity resulting from the limited number of ions. In contrast, the sufficient numbers of ions in PIGT$_{x100}$ provide high ionic conductivity and enable fast formation of electric double layers and subsequent doping. The hysteresis of transfer curves also mirrors this observation (Figure S11, Supporting Information).

To determine the response time, on/off transient behavior was investigated by measuring I_d after turning V_g on and off. The voltage drop at the resistance across the source and drain was recorded with an oscilloscope and converted to the transient current (for details, see Experimental Section). The off current was directly premeasured and indicated as dotted lines in Figures 4c,d and Figures S12 and S13, Supporting Information. PIGT$_{x100}$ shows a remarkable response time of ≈20 µs for both turning on and off. This is the fastest response time among electrochemical-based accumulation mode transistors ever reported.[6f] Furthermore, the actual response time is even faster than 20 µs because this time scale is already below the time

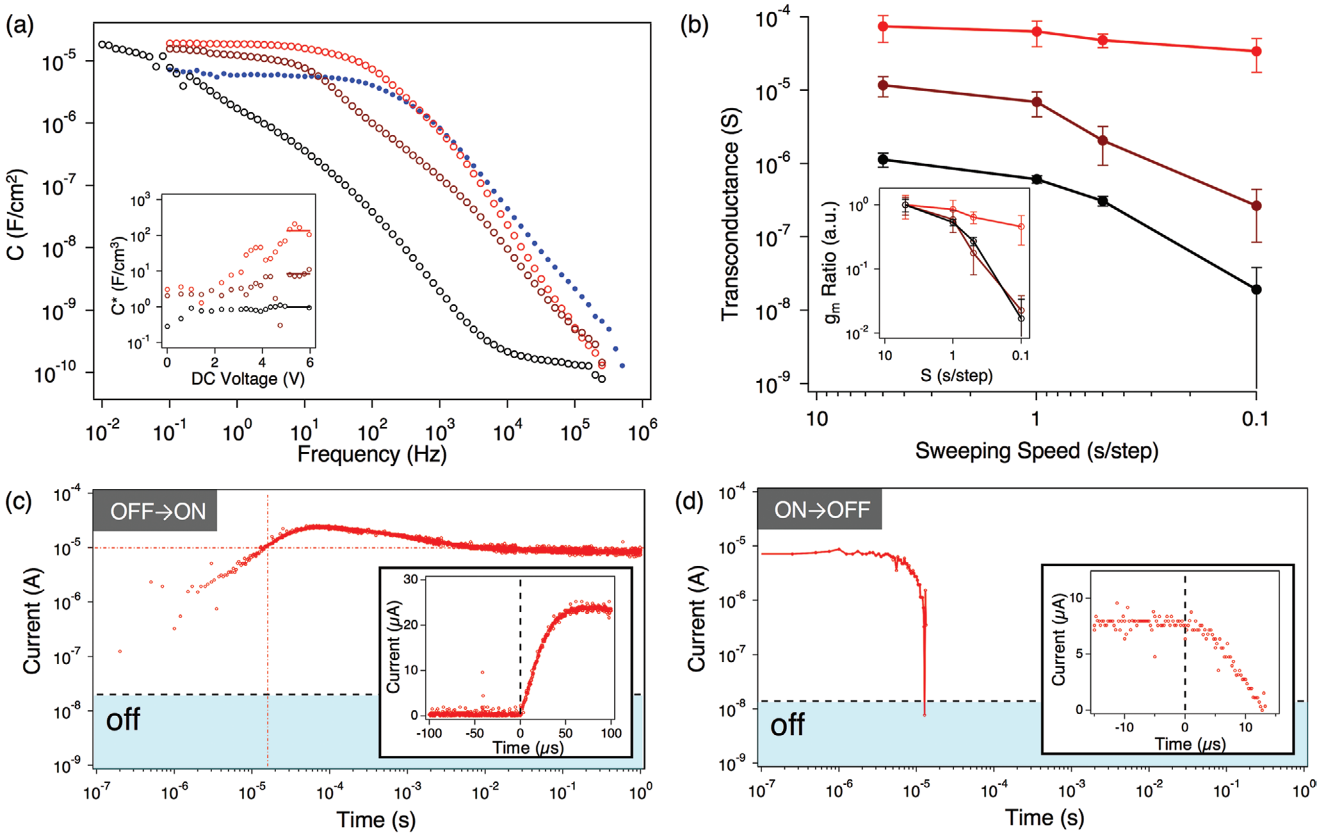

Figure 4. a) Capacitance per area at $V_{DC} = 0$ V as a function of the frequency for π-ion gel$_{x1}$ (black), π-ion gel$_{x10}$ (dark red), π-ion gel$_{x100}$ (red), and a pure IL (blue). The inset shows capacitance per volume as a function of DC voltage. The solid lines are saturated values of volumetric capacitance. b) The transconductance of PIGT$_{x100}$ (red), PIGT$_{x10}$ (dark red), and PIGT$_{x1}$ (black) as a function of the sweeping speed. The inset displays the transconductance ratio normalized at 5 s/step. Transient currents after turning the gate voltage of −5.1 V c) on and d) off. The insets depict the linear time scale of ±100 µs or ±20 µs.

resolution of the measuring apparatus (Figure S14, Supporting Information). In contrast, PIGT$_{x1}$ and PIGT$_{x10}$ respond in a range of several hundred milliseconds to several tens of seconds, even slower than conventional OECTs.[3b,e] Transient gate currents of PIGT$_{x10}$ and PIGT$_{x1}$ indicate that electric double layers form well prior to the device response, suggesting that doping process dominates the device response (Figure S15, Supporting Information). We attribute the fast response of PIGT$_{x100}$ to the large interface and the high ionic conductivity, which are associated with the distinct minute structures of π-ion gels and the device configuration. In comparison to OECTs, PIGT can skip the injection of ions into an active layer. Hence, the device structure of PIGT$_{x100}$ is beneficial to serve excess amount of anions that not only form electric double layers, but also accelerate doping process by compensating hole-carriers. Table S5, Supporting Information, summarizes the response speed of PIGTs. It should be noted that we are not the first group to have aimed at pre-distributing ions into semiconducting layers of transistors. Sariciftci et al. have already attempted using a mixed film of an electrolyte and a conjugated polymer as an active layer of OFET, inspired by light-emitting electrochemical cells.[8] Although the mobility increased threefold, drastic improvement of the general performance was not observed. The device still requires a dielectric layer as OFETs. In their work, the mixture ratio of conjugated polymer and ions (5:1) is far smaller than that of our PIGT$_{x100}$ (1:100). We have demonstrated that PIGT is operative without a dielectric layer and that the IL ratio plays a crucial role in response time and transconductance. Therefore, the gelation strategy that can access films containing 99% IL is a powerful tool. The low stability in ambient is definitely an issue for the wide scope of practical applications. However, this issue is rather related to the molecular properties of the materials used than the general concept of PIGT. An encapsulation—as commonly used for other organic electronic devices—or molecular engineering, that we have not explored in this work, should be able to solve this problem and develop PIGTs further.

To summarize, a new class of supramolecular transistors, PIGTs, was demonstrated. We clarified that the internal structure of our π-ion gel is a nanofiber network of PPE that encloses a 100 times larger amount of IL at maximum. This in situ π-ion gel is capable of acting as both an active layer and an internal gate capacitor; the integrated IL serves as a capacitor to fibers and triggers conductivity. The device displays volumetric currents as well as high transconductance (133 µS), retaining an on/off ratio (≈3.7×10^4) and a mobility (4.2×10^{-2} cm^2 V^{-1} s^{-1}) comparable to those of PPE supramolecular devices. The distinct nanodomains of PPE and IL in the π-ion gel maximize the area of the interface, whereas the nanospaces between fibers ensure massive ionic paths. As a result, PIGT displays the fastest response time ever reported (<20 µs) for accumulation-mode electrochemical-based transistors. We offer a rational platform for device manufacturing to maximize the macroscopic device performance by the use of microscopic supramolecular assemblies, providing a new method in the interdisciplinary field of supramolecular chemistry and organic electronics. The flexibility of gels and the absence of a dielectric layer are additional advantages of PIGTs that make them applicable in flexible printed electronics.

Supporting Information

Supporting Information is available from the Wiley Online Library or from the author.

Acknowledgements

The authors acknowledge Mr. Taishi Kanamaru for the CFM observation. S.K. is grateful to DAAD (91612715) and JSPS KAKENHI (Grant Number JP20J00845) for the scholarship and financial support.

Open access funding enabled and organized by Projekt DEAL.

Conflict of Interest

The authors declare no conflict of interest.

Keywords

π-gels, conjugated polymers, ionic liquids, PPE, supramolecular transistors

Received: September 7, 2020
Revised: November 18, 2020

[1] a) H.-J. Kim, T. Kim, M. Lee, *Acc. Chem. Res.* **2011**, *44*, 72; b) S. Yagai, Y. Kitamoto, S. Datta, B. Adhikari, *Acc. Chem. Res.* **2019**, *52*, 1325.

[2] a) T. Aida, E. W. Meijer, S. I. Stupp, *Science* **2012**, *335*, 813; b) F. S. Kim, G. Ren, S. A. Jenekhe, *Chem. Mater.* **2011**, *23*, 682; c) L. Zang, Y. Che, J. S. Moore, *Acc. Chem. Res.* **2008**, *41*, 1596; d) T. Kitamura, S. Nakaso, N. Mizoshita, Y. Tochigi, T. Shimomura, M. Moriyama, K. Ito, T. Kato, *J. Am. Chem. Soc.* **2005**, *127*, 14769.

[3] a) D. K. Kumar, J. W. Steed, *Chem. Soc. Rev.* **2014**, *43*, 2080; b) S. S. Babu, V. K. Praveen, A. Ajayaghosh, *Chem. Rev.* **2014**, *114*, 1973; c) F. Würthner, C. Bauer, V. Stepanenko, S. Yagai, *Adv. Mater.* **2008**, *20*, 1695; d) A. Ajayaghosh, S. J. George, *J. Am. Chem. Soc.* **2001**, *123*, 5148; e) V. S. Nair, R. D. Mukhopadhyay, A. Saeki, S. Seki, A. Ajayaghosh, *Sci. Adv.* **2016**, *2*, e1600142; f) W. Y. Huang, S. Matsuoka, T. K. Kwei, Y. Okamoto, *Macromolecules* **2001**, *34*, 7166; g) S. Yagai, M. Ishii, T. Karatsu, A. Kitamura, *Angew. Chem., Int. Ed.* **2007**, *46*, 8005.

[4] a) S. S. Babu, S. Prasanthkumar, A. Ajayaghosh, *Angew. Chem., Int. Ed.* **2012**, *51*, 1766; b) J.-P. Hong, M.-C. Um, S.-R. Nam, J.-I. Hong, S. Lee, *Chem. Commun.* **2009**, 310; c) W.-W. Tsai, I. D. Tevis, A. S. Tayi, H. Cui, S. I. Stupp, *J. Phys. Chem. B* **2010**, *114*, 14778; d) S. Diring, F. Camerel, B. Donnio, T. Dintzer, S. Toffanin, R. Capelli, M. Muccini, R. Ziessel, *J. Am. Chem. Soc.* **2009**, *131*, 18177; e) H. Dong, S. Jiang, L. Jiang, Y. Liu, H. Li, W. Hu, E. Wang, S. Yan, Z. Wei, W. Xu, X. Gong, *J. Am. Chem. Soc.* **2009**, *131*, 17315; f) Y.-S. Guan, Y. Qin, Y. Sun, C. Wang, W. Xu, D. Zhu, *Chem. Commun.* **2015**, *51*, 12182.

[5] a) S. Kushida, E. Smarsly, L. Veith, I. Wacker, R. R. Schröder, U. H. F. Bunz, *Macromolecules* **2017**, *50*, 7880; b) S. Kushida, S. Kebrich, E. Smarsly, K.-P. Strunk, C. Melzer, U. H. F. Bunz, *ACS Appl. Mater. Interfaces* **2020**, *12*, 38483.

[6] a) H. S. White, G. P. Kittlesen, M. S. Wrighton, *J. Am. Chem. Soc.* **1984**, *106*, 5375; b) J. Rivnay, S. Inal, A. Salleo, R. M. Owens, M. Berggren, G. G. Malliaras, *Nat. Rev. Mater.* **2018**, *3*, 17086; c) S. Inal, G. G. Malliaras, J. Rivnay, *Nat. Commun.* **2017**, *8*, 1767; d) S. Inal, J. Rivnay, P. Leleux, M. Ferro, M. Ramuz, J. C. Brendel, M. M. Schmidt, M. Thelakkat, G. G. Malliaras, *Adv. Mater.* **2014**, *26*, 7450; e) A. Laihoa, L. Herlogssona, R. Forchheimerb, X. Crispina, M. Berggren, *Proc. Natl Acad. Sci. U. S. A.* **2011**, *108*, 15069; f) A. Giovannittia, D.-T. Sbirceaa, S. Inal, C. B. Nielsena, E. Bandielloe, D. A. Hanifif, M. Sessoloe, G. G. Malliarasb, I. McCulloch, J. Rivnay, *Proc. Natl Acad. Sci. U. S. A.* **2016**, *113*, 12017; g) J. D. Yuen, A. S. Dhoot, E. B. Namdas, N. E. Coates, M. Heeney, I. McCulloch, D. Moses, A. J. Heeger, *J. Am. Chem. Soc.* **2007**, *129*, 14367; h) J. Rivnay, P. Leleux, M. Ferro, M. Sessolo, A. Williamson, D. A. Koutsouras, D. Khodagholy, M. Ramuz, X. Strakosas, R. M. Owens, C. Benar, J.-M. Badier, C. Bernard, G. G. Malliaras, *Sci. Adv.* **2015**, *1*, e1400251; i) G. D. Spyropoulos, J. N. Gelinas, D. Khodagholy, *Sci. Adv.* **2019**, *5*, eaau7378.

[7] a) S. Schmid, A. K. Kast, R. R. Schröder, U. H. F. Bunz, C. Melzer, *Macromol. Rapid Commun.* **2014**, *35*, 1770.

[8] C. Yumusak, M. Abbas, N. S. Sariciftci, *J. Lumin.* **2013**, *134*, 107.